The TOWER
Undergraduate Research Journal
gttower.org

Dynamics of an Acoustically Excited Swirl Flame

HSIN-HSIAO MA

We present an experimental investigation of the dynamics of an acoustically excited swirl combustor. Simultaneous measurements were taken of the acoustic pressure, mean velocity, CH and OH* radical chemiluminescence, and OH concentrations through planar laser induced fluorescence (PLIF) over a range of forcing frequencies, amplitudes and nozzle exit velocities. As the flame response grows linearly and monotonically with increasing forcing amplitude, the flame's behavior becomes more complex at higher levels. The observed dynamics of the flame to some extent occur simultaneously, resulting from a combination of at least five flame/flow processes: (1) the oscillating velocity of the annular jet, oscillations in (2) position and (3) strength of the vortex breakdown bubble and separation bubble, (4) unsteady liftoff of the flame, and (5) an oscillating turbulent flame speed.*

INTRODUCTION

This work is motivated by combustion instabilities in lean (oxygen rich), premixed combustors and continues recent studies by Thumuluru, S.K., Bobba, M.K., & Lieuwen, T. (2007). Combustion instabilities are characterized by pressure oscillations of the acoustic modes of the combustor (Lee & Santavicca, 2003; Richards, Straub, & Robey, 2003). Every object has a natural frequency that it oscillates at when disturbed. For example: blowing into a bottle filled a quarter of the way with liquid would yield a different sound than blowing into the same bottle half-filled. The natural frequency is determined by the materials and the geometry involved. The acoustics produced from the disturbance cause instabilities in the combustion process, which can results in structural vibrations, thrust oscillations, and enhanced heat transfer that can substantially reduce the life of the combustor. In addition, this could also compromise efficiency and the surrounding environment, forcing the combustor to be operated at lower levels and can even cause catastrophic failure. Figure 1 is a pictorial representation of the complex, non-monotonic, acoustic dynamics of the combustion zone. To simulate the disturbances, two speakers were used to produce a driving amplitude, H(A). D(A), the damping amplitude represents losses that dampen the driving (sound) amplitude within the system. The flame's heat release response, which is the amount of heat released by the flame due to a disturbance, at first increases linearly over a certain range

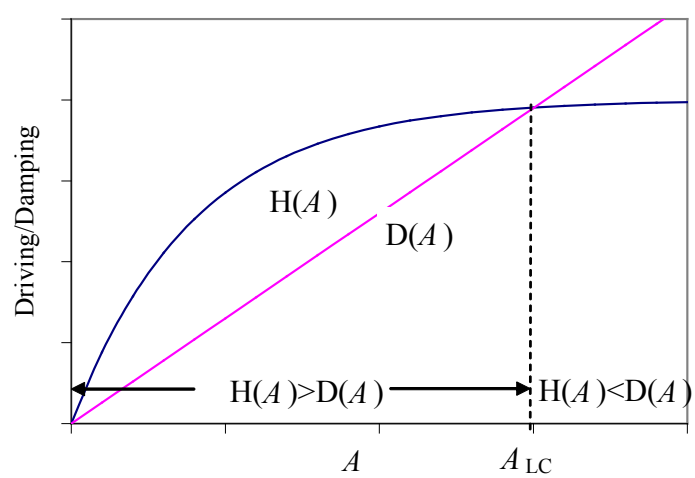

Figure 1. Qualitative plot showing amplitude dependence of the disturbance driving, H(A), and damping, D(A). Adapted from Thumuluru, Ma et al., (2007).

Contact email: *hma6@gatech.edu*
Advisors: Tim Lieuwen, PhD, Sai Kumar Thumuluru
School: School of Aerospace Engineering
Georgia Institute of Technology

of low amplitudes, then saturates (levels out) at higher amplitudes (Lieuwen, 2002 and Dowling, 1997). The saturation is analogous to the following in the bottle setup noted above: increasing excitation amplitude (blowing harder) into the bottle would yield higher response (louder sound) until a certain input amplitude is reached. At this point, the response amplitude will no longer increase with an increase in input; at some point blowing into the bottle harder will no longer produce a louder sound. The location of this point is also known as the limit-cycle (ALC). The low amplitude linear dynamics control the balance between driving and damping of the disturbances while the high amplitude nonlinear dynamics control the location of the limit-cycle.

Combustion instabilities spontaneously occur when the forcing of the oscillations from the combustion processes is greater than the dampening of oscillations. The limit-cycle amplitude (ALC) describes the point where the driving force equals the damping force (i.e. steady-state), causing saturation if forcing continues to increase. Identifying this steady-state point is essential because it could serve as a threshold of maximum efficiency at safe operating conditions for combustors. Proceeding past the threshold could result in some of the failures listed above along with the possibility of flame blowoff (flame is extinguished) or flashback (flow goes back into the nozzle). Predicting the limit-cycle entails a deep understanding of how the flame's heat release is influenced by the fluctuation of the excitation amplitude. The key objective of this work is to characterize the physics behind the mechanisms causing such instabilities.

EXPERIMENTAL SETUP

The experimental combustor is swirl stabilized with a center-body and operates at atmospheric pressure and 10-20 KW thermal power. Swirl stabilizing the flow is achieved by passing the flow through a swirler, which produces a toroidal flow structure that has stabilizing properties. The center-body is a physical body that contains the swirler, the ducts leading from the swirler, and is the body the flame sits on. Figure 2 is a schematic of the combustor setup. The fuel (natural gas) and air were premixed upstream of a choke point to prevent the occurrence of fuel/air ratio oscillations. The equivalence ratio, also known as the air-fuel ratio, was maintained throughout the experiments at a constant value of 0.8. The premixed fuel and air were passed through a flow swirler with a 40° swirl angle. The resulting flow was then passed through the center-body then expanded into a quartz tube of a 70 mm diameter and 190 mm length. This specific length was selected to avoid the natural frequency of the quartz tube and thus, prevent any self-excited oscillations. Acoustic oscillations are introduced using two amplifiers (Radio Shack MPA – 101 100 Watts) connecting to two drivers (SK144 100 Watt speakers), which were mounted upstream of the combustor. Two pressure transducers (Model 211B5 Kistler) positioned downstream of the swirler, located 5.85 cm and 7 cm upstream of the nozzle, are used to determine the acoustic velocity at the nozzle exit using the two microphone method (Allam & Åbom, 2005).

In order to provide some context for interpreting the results of this study, Figure 3 has been provided to depict common fluid mechanical processes and basic flame configurations. Figure 3(a) breaks down the combustion zone into three main regions: (1) The outer recirculation zone (ORZ), which is a toroidal re-circulating regime generated by the rapid expansion of the jet into the combustor, (2) the inner recirculation zone (IRZ), due to vortex breakdown accompanying the swirl-

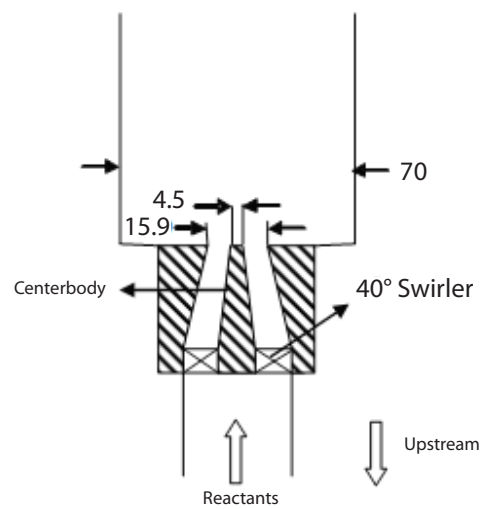

Figure 2. Combustor schematic (all dimensions are in mm). Adapted from Thumuluru, Ma et al., (2007).

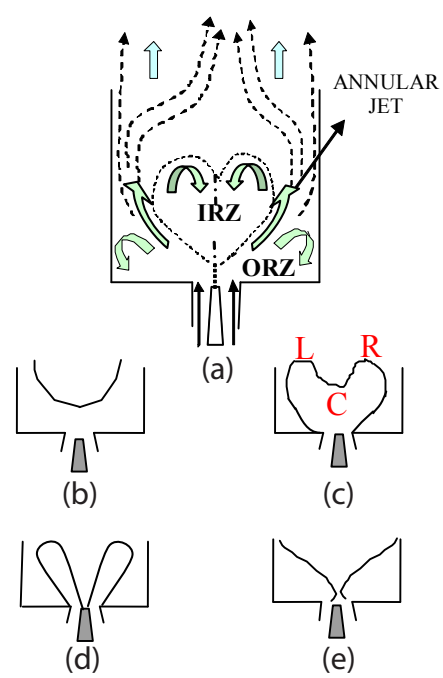

Figure 3. (a) Common fluid mechanical processes. (b) – (e) Common flame structures. Adapted from Thumuluru, Ma et al., (2007).

ing flow, and (3) the high velocity, annular fluid jet that divides these regions. Figure 3(b) – (e) depicts common flame configurations that are heavily dependent on the equivalence ratio and flow velocity. Disturbances to the velocity before the nozzle exit alter the velocity of the annular fluid jet, which causes the flame to surge up and down axially. This causes both the ORZ and IRZ strength to fluctuate and its location to shift back and forth.

Phased locked OH Planar Laser Induced Fluorescence (PLIF) was used to visualize the spatial dynamics of the flame while measurements of the global CH* and OH* radical chemiluminescence with photomultipliers (PMT) were used to characterized the heat release fluctuations. A schematic of the laser system is shown in Figure 4 and detailed specifications are given in Thumuluru, Bobba et al. (2007).

The key limiter of using the PLIF images is that the flame edges are captured manually and consequently subjected to biases. Every edge detection software applied to the flame images returns with several errors due to the complexity of each picture; however, determination of the flame edge manually is trivial in most cases, except when the flame reflects itself off of the combustor walls and/or where there is back mixing of OH laden products. In the latter case, the OH gradient helps distinguish between whether the OH levels correspond to a flame or a product.

IMAGE ANALYSIS

To trace the changes in the flame structure, OH PLIF images were recorded and analyzed for specific conditions within the range of: (1) frequency: 100 Hz to 410 Hz and (2) excitation amplitude: 100 mV to 1500 mV. The interpretation of these images is limited by the fact that they are only two-dimensional projections of a highly three-dimensional flow, offering only a sliver of the combustion zone. This limited view into the combustion zone only reveals interactions on a two dimensional plane, while the flow is changing and interacting three dimensionally. Also, despite the images being phased locked, the images are actually taken several cycles apart and do not represent consecutive cycles.

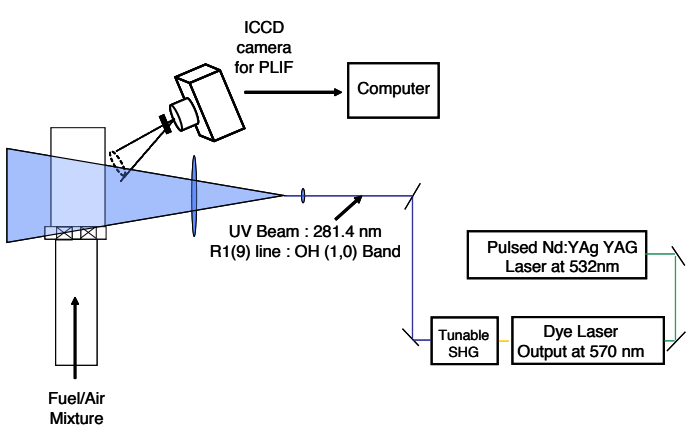

Figure 4. Schematic of the OH PLIF setup. Adapted from Bellows et al., (2006).

A typical set of PLIF images of a flame were taken at six different phases of an acoustic cycle at selected excitation amplitudes (produced by the speakers) as shown in Figure 5. The forcing frequency here was 140 Hz and the phase angles correspond to the phase angles within an acoustic cycle. The Reynolds number (ratio of inertial forces to viscous forces) was defined at the nozzle exit at 44,000. The ratio u'/u_o is the acoustic velocity to the mean velocity of the flow. This ratio provides a valuable insight into the magnitude of oscillations in the flow with zero being no fluctuations. As excitation amplitude increases, u'/u_o will also increase. The flame shape at this condition is similar to Figure 3(c) where the flame is attached on the outer walls. Note the nozzle is located at the bottom of each image.

Figures 5(a) and (b) are snapshots of the flame at low excitation amplitudes, which would fall under the linear regime of the flame response as shown by Figure 1 with the H(A) curve. The curve rises linearly before turning and saturating. Notice that in the IRZ region, the flame is almost attached to the centerbody. The significance of this phenomenon is explained later in this section. Figure 5(c) and (d) show the flame under large excitation amplitudes where the flame response saturates and recovers, respectively. In Figure 5(d) specifically, the flame edge in the IRZ region is far away at phase angle 120°, stabilizes at phase angles 180° and 240°, and recovers at 300°. In general, Figure 5 provides an illustration of the flame as it surges back and forth axially, due to oscillating flow velocity in the annular jet region shown in Figure 3(a). A closer look into this phenomenon is well illustrated in Figure 5(d). As the excitation amplitude grows, the overall level of fluctuation of the flame length grows, which can be seen in the ORZ region as the flame edge shifts axially.

Applying this process of image analysis over a range of conditions, it was observed and cataloged that there are five basic flame and/or flow processes. These processes are the following:

Fluctuating annular jet velocity. As noted above, oscillations in flow velocity cause perturbations in the annular jet velocity between the IRZ and ORZ, causing a fluctuation in flame length.

Vortex rollup. The oscillating shear in the inner and outer re-circulation zones generates vortical structures whose strength and size are a function of the perturbation amplitudes. These vortices roll up the flame and cause rapid destruction of the flame area. Figure 6 illustrates that significant vortex rollup occurs in both the IRZ (left) and the ORZ (right). Figure 5(c) shows the evolution of a vortex rollup through a cycle of phase angles.

Unsteady Liftoff. The flame's stabilization point is heavily de-

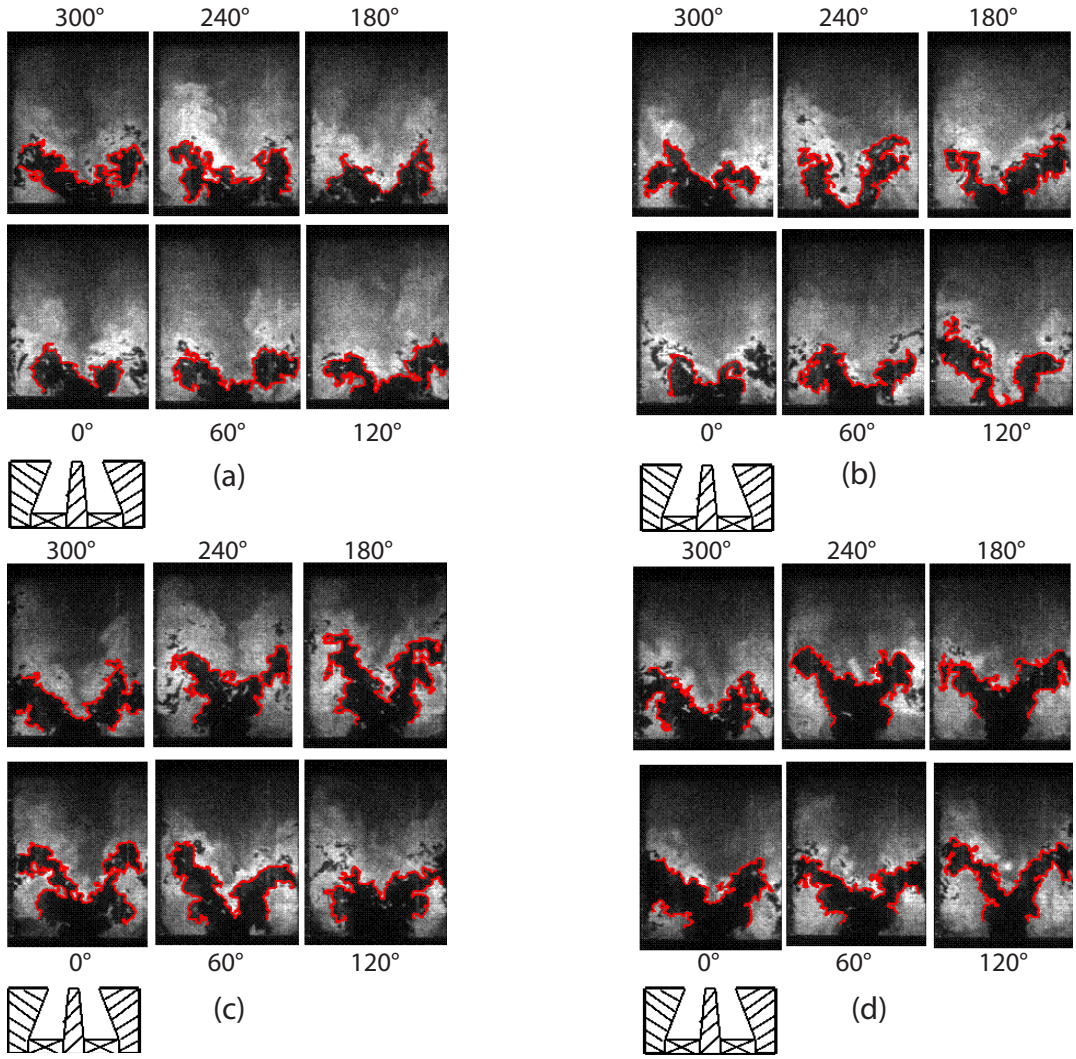

Figure 5. OH PLIF images showing flame structure at the forcing frequency of 140 Hz, R_e = 44,000 and amplitudes of (a) u'/u_o = 0.07, (b) u'/u_o = 0.1, (c) u'/u_o = 0.17 & (d) u'/u_o = 0.24. Figure adapted from Thumuluru, Ma et al., (2007).

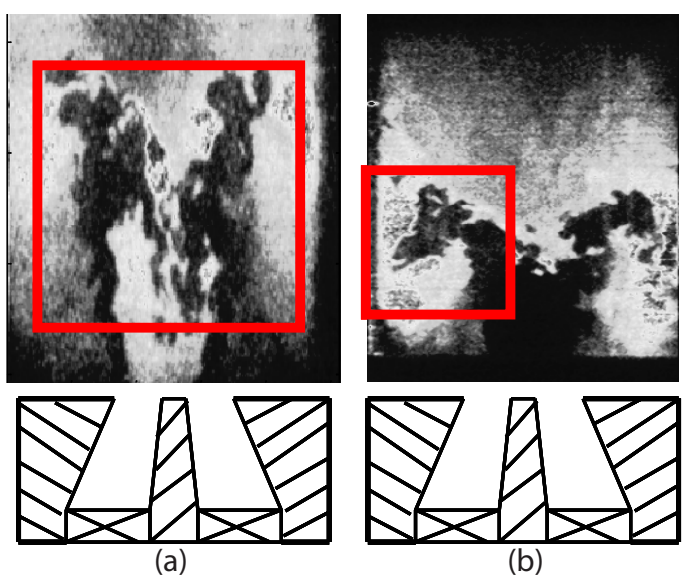

Figure 6. PLIF images showing vortex rollup in IRZ (left) and ORZ (right) at forcing frequency of (a) 130 Hz, R_e = 21,000, u'/u_o = 0.9 & (b) 210 Hz, R_e = 44,000, u'/u_o = 0.2. Adapted from Thumuluru, Ma et al., (2007).

pendent on the excitation amplitude and can be pushed downstream. At higher excitation amplitudes, the flame extinguishes locally between the swirler exits as shown in Figure 7 and restabilizes downstream. Notice, at 0° phase angle, the flame edge is clearly attached to the center-body while at 225° phase angle the flame edge has completely lifted off. The bulk of the heat release has moved away from the IRZ and towards the walls of the combustor. This phenomenon is apparently the cause of the saturation (non-linear regime) of the flame response to excitation. When the flame is attached to the center-body as shown in Figure 3(d) and (e), the flame edge grows linearly with excitation amplitude and stretches axially. Once the flame detaches and is blown downstream as shown in Figure 3(b) and (c), the flame responds to the higher excitation amplitude by shifting up and down in bulk. This is accompanied with a decrease in flame area, which results in lower heat release.

Vortex breakdown bubble movement. The vortex breakdown bubble also known as the IRZ moves up and down axially and changes shape with forcing as seen in Figure 8 taken at 410 Hz.

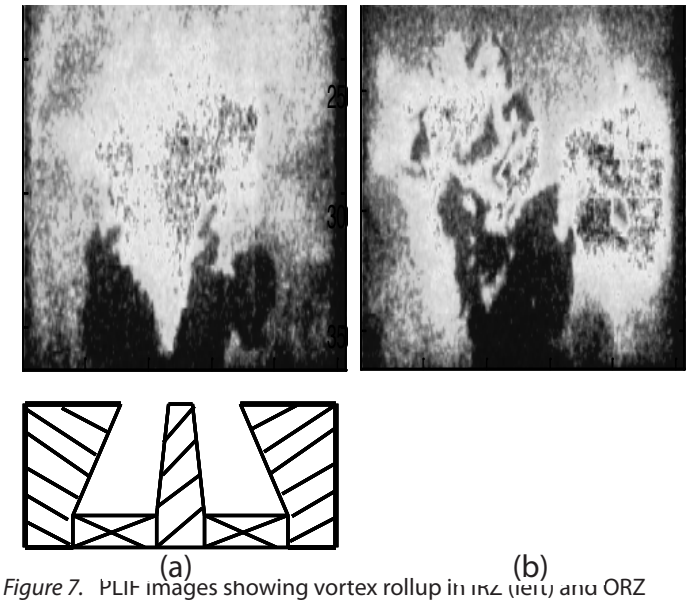

Figure 7. PLIF images showing vortex rollup in IRZ (left) and ORZ (right) at forcing frequency of (a) 130 Hz, R_e = 21,000, u'/u_o = 0.9 & (b) 210 Hz, R_e = 44,000, u'/u_o = 0.2. Adapted from Thumuluru, Ma et al., (2007).

Comparing Figure 5 and Figure 8, it appears that the recirculation bubble responds to frequencies instead of excitation amplitude.

Turbulent flame speed oscillations. The turbulent flame speed (speed of propagation) of the unburned reactants varies throughout the cycle of phase angles. In a previous qualitative observation by Bellows, Bobba, Seitzman, & Lieuwen (2006), it was observed that the flame topology varies with excitation amplitude. In Figure 5, where the excitation amplitudes are small, the amount of "flame wrinkling" (flame physically changes to appear as if it were wrinkled) fluctuates throughout an acoustic cycle as the excitation amplitude increases. In Figure 6(b) and Figure 7 at a phase angle of 225° where the excitation amplitudes are high, the flame wrinkling becomes virtually unpredictable. This implies that the turbulent flame speed oscillates with a fluctuation level that increases with the excitation amplitude.

CONCLUSION

The results presented show that the observed dynamics to some extent occur simultaneously, resulting from a combination of at least five flame/flow mechanical processes – the oscillating velocity of the annular jet, oscillations in position and strength of the vortex breakdown bubble and separation bubble, unsteady liftoff of the flame, and an oscillating turbulent flame speed. These five flame/flow mechanical processes shed valuable insight into the interactions within the combustion zone. These results cannot be applied directly to industry, but they are the fundamental building blocks of a more in-depth investigation. A key conclusion from this study is that investigation into flame

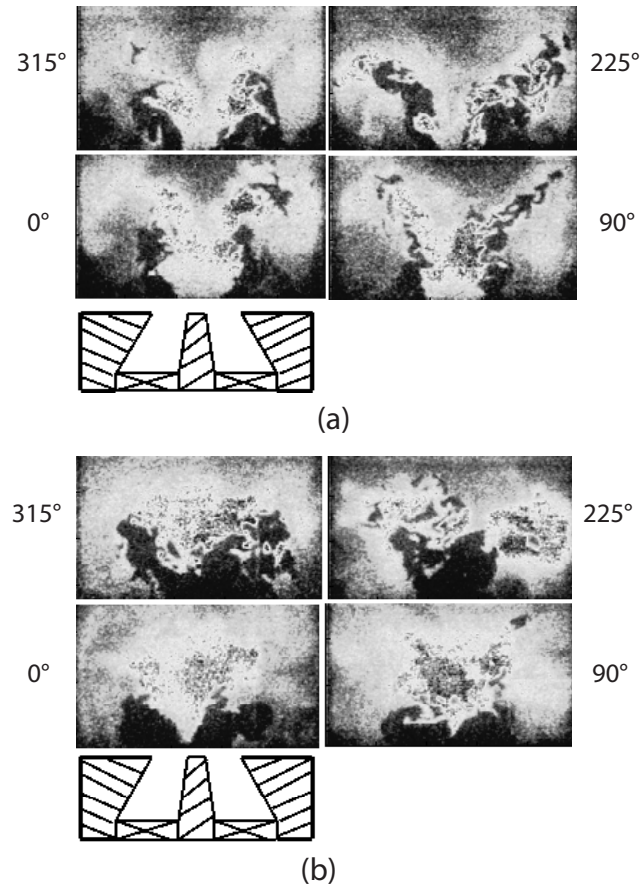

Figure 8. PLIF images at forcing frequency of 410 Hz, R_e = 21,000, (a) u'/u_o = 0.2 (b) u'/u_o = 0.6. Adapted from Thumuluru, Ma et al., (2007).

dynamics through pattern analysis is not enough. Further work includes taking particle image velocimetry (PIV) to capture the velocity field of the flame. PIV is an optical method used to measure velocity fields and other properties in fluids. The flow is seeded (particles are introduced into the flow) with small reflective particles that reflect light created by a laser. The reflected light is then captured on camera every few milliseconds, revealing the velocity magnitude and direction of the flow. The PIV method should provide more quantitative data to integrate these fluid mechanic descriptions into phenomenological descriptions of the phenomenon.

ACKNOWLEDGMENTS

The author would like to thank his advisors Sai Kumar Thumuluru and Tim Lieuwen for their guidance.

REFERENCES

Allam, S., & Åbom, M. (2005). Investigations of damping and radiation using full plane wave decomposition in ducts. *Journal of Sound and Vibration*, *292*(3–5), 519–534.

Bellows, B. D., Bobba, M. K., Seitzman, J. M., & Lieuwen, T. (2006). Nonlinear flame transfer function characteristics in a swirl-stabilized combustor. *Journal for Engineering of Gas Turbines and Power*, 129(4), 954–961.

Dowling, A. P. (1997). Nonlinear self-excited oscillations of a ducted flame. *Journal of Fluid Mechanics*, *346*, 271 – 290.

Lee, J., & Santavicca, D. (2003). Experimental diagnostics for the study of combustion instabilities in lean premixed combustors. *Journal of Propulsion and Power*, *19*(5), 735–750.

Lieuwen, T., & Zinn, B. T. (2002). Experimental investigation of limit-cycle oscillations in an unstable gas turbine combustor. *Journal of Propulsion and Power*, *18*(1), 61–67.

Richards, G., Straub, D., & Robey, E. (2003). Passive control of combustion dynamics in stationary gas turbines. *Journal of Propulsion and Power*, *19*(5), 795–810.

Thumuluru, S. K., Bobba, M. K., & Lieuwen, T. (2007). Mechanisms of Nonlinear of a Swirl Flame to Harmonic Excitation. *ASME paper*, GT 2007-27932.

Thumuluru, S. K., Ma, H. H., & Lieuwen, T. (2007). Measurements of the Flame Response to Harmonic Excitation in a Swirl Combustor, *AIAA paper*, AIAA 2007-0845.